Biophysical Journal Volume 109 October 2015 1630–1638

Article

The Effect of Membrane Lipid Composition on the Formation of Lipid Ultrananodomains

Priyadarshini Pathak[1] and Erwin London[1,*]
[1]Department of Biochemistry and Cell Biology, Stony Brook University, Stony Brook, New York

ABSTRACT Some lipid mixtures form membranes containing submicroscopic (nanodomain) ordered lipid domains (rafts). Some of these nanodomains are so small (radius <5 nm) that they cannot be readily detected with Förster resonance energy transfer (FRET)-labeled lipid pairs with large Ro. We define such domains as ultrananodomains. We studied the effect of lipid structure/composition on the formation of ultrananodomains in lipid vesicles using a dual-FRET-pair approach in which only one FRET pair had Ro values that were sufficiently small to detect the ultrananodomains. Using this approach, we measured the temperature dependence of domain and ultrananodomain formation for vesicles composed of various mixtures containing a high-T_m lipid (brain sphingomyelin (SM)) or dipalmitoyl phosphatidylcholine (DPPC)), low-T_m lipid (dioleoylphosphatidylcholine (DOPC) or 1-palmitoyl 2-oleoyl phosphatidylcholine (POPC)), and a lower (28 mol %) or higher (38 mol %) cholesterol concentration. For every lipid combination tested, the thermal stabilities of the ordered domains were similar, in agreement with our prior studies. However, the range of temperatures over which ultrananodomains formed was highly lipid-type dependent. Overall, vesicles that were closest to mammalian plasma membrane in lipid composition (i.e., with brain SM, POPC, and/or higher cholesterol) formed ultrananodomains in preference to larger domains over the widest temperature range. Relative to DPPC, the favorable effect of SM on ultrananodomain formation versus larger domains was especially large. In addition, the favorable effect of a high cholesterol concentration, and of POPC versus DOPC, on the formation of ultrananodomains versus larger domains was greater in vesicles containing SM than in those containing DPPC. We speculate that it is likely that natural mammalian lipids are tuned to maximize the tendency to form ultrananodomains relative to larger domains. The observation that domain size is more sensitive than domain formation to membrane composition has implications for how membrane domain properties may be regulated in vivo.

INTRODUCTION

Ternary mixtures of lipids with a high gel-to-liquid disordered (Ld) transition temperature, low gel-to-Ld/liquid crystalline transition temperature, and cholesterol can form bilayers with coexisting Ld and liquid-ordered (Lo) domains (1). The behavior of such mixtures is of interest because it is believed that Lo domains (lipid rafts) can exist in plasma membranes. Lipid rafts have been proposed to carry out a large range of biological functions (2–4). Questions concerning the effect of lipid composition on domain formation are important because they can provide insights into the conditions under which membrane domains will form spontaneously, as well as the physical properties of the domains.

Lipid domain size is one physical property that can have an important impact on domain function (see Discussion). It is known that for some lipid compositions, ordered domains exist as large-scale phases of micron size, whereas in other cases they exist as nanodomains, which are too small to detect by ordinary light microscopy (5–7). Liquid-ordered nanodomains have been found in sizes of just a few nanometers (5,6,8). Some factors that influence domain size have been identified, such as the contribution of a hydrophobic mismatch between ordered and disordered domain thicknesses to line tension (7). Nevertheless, although possible mechanisms have been proposed (9), there is no agreement as to what drives the formation of nanodomains in place of large-scale phase separations.

Much of the confusion concerning when rafts are present in living cells may be due to the difficulty of detecting nanodomains, and especially very small (ultra) nanodomains, as few methods can detect lipid segregation on such a scale. Förster resonance energy transfer (FRET) is one such method (6,8,10–13). However, even FRET, which has a detection limit on the order of 5 nm or less depending on the donor-acceptor pair, can fail to detect an ultrananodomain if a donor-acceptor pair with a large Ro is used (8).

In a previous study, we found that vesicles composed of mixtures of brain sphingomyelin (SM), 1-palmitoyl 2-oleoyl phosphatidylcholine (POPC), and cholesterol form nanodomains with a size that is highly temperature dependent (8). In the work presented here, we explored the effect of lipid composition on domain size in what we define as the ultrananodomain range, i.e., domains with a width/diameter of less than ~10–12 lipid molecules (which for a circular domain would contain on the order of 100 lipids per leaflet or less).

Submitted April 14, 2015, and accepted for publication August 21, 2015.
*Correspondence: erwin.london@stonybrook.edu
Editor: Paulo Almeida.

0006-3495/15/10/1630/9
http://dx.doi.org/10.1016/j.bpj.2015.08.029

For this purpose, we used a dual-FRET-pair approach to detect ultrananodomain formation as a function of lipid composition. This method estimates the domain size by making use of two domain-detecting FRET measurements with different size-detection thresholds, i.e., using FRET pairs with different Ro values. When both measurements detect domains (the domains are larger than the Ro of both FRET pairs used), the domains are larger than that of the measurement with the highest threshold (i.e., the largest Ro), whereas when only the low-threshold measurement detects domains (i.e., the domains are smaller than Ro for the FRET pair with the largest Ro), their size is between the two detection threshold values (8). When neither method detects domains, they are either absent or smaller than that of the measurement with the lowest threshold. We find that the lipid composition has a strong influence on the formation of nanodomains, and that natural lipid compositions seem to favor the formation of ultrananodomains. We also discuss the choice of conditions for FRET experiments that will allow the most robust detection of the formation of nanodomains.

MATERIALS AND METHODS

Materials

Porcine brain SM (bSM), POPC, 1,2-dioloeyl-phosphatidylcholine (DOPC), 1,2-dipalmitoyl-phosphatidylcholine (DPPC), cholesterol, and fluorescent headgroup-labeled lipids (1,2-dipalmitoylphosphatidylethanolamine-N-(7-nitro-2-1,3-benzoxadiazol-4-yl) (NBD-DPPE), 1,2-dipalmitoylphosphatidylethanolamine-N-(1-pyrenesulfonyl) ammonium salt (pyrene-DPPE), and 1,2-dioleoylphosphoethanolamine-N-(lissamine rhodamine B sulfonyl) (rhodamine-DOPE)) were purchased from Avanti Polar Lipids (Alabaster, AL) or Invitrogen. Lipids and probes were dissolved in chloroform and stored at −20°C. The concentrations of nonfluorescent lipids were determined by dry weight and those of fluorescent lipids were determined by absorbance using ε (NBD-DPPE) 21,000 $M^{-1}cm^{-1}$ at 460 nm, ε (pyrene-DPPE) 35,000 $M^{-1}cm^{-1}$ at 350 nm, and ε (rhodamine-DOPE) 88,000 $M^{-1}cm^{-1}$ at 560 nm.

Vesicle preparation

Multilamellar vesicles were prepared in a manner similar to that described previously (8). Briefly, lipids and fluorophores were pipetted in glass tubes, dried under nitrogen, redissolved in 20 μL of chloroform, and redried under nitrogen. They were then dried under high vacuum for 2 h and finally dispersed in 975 μL of 70°C phosphate-buffered saline (PBS) (1 mM KH_2PO_4, 10 mM Na_2HPO_4, 137 mM NaCl, and 2.7 mM KCl, pH 7.4). The final samples contained 500 μM of unlabeled lipid and, for FRET studies, 0.1 mol % NBD-DPPE or 0.05 mol % pyrene-DPPE as donor, with or without 2 mol % rhodamine-DOPE as acceptor. Background samples lacking fluorescent lipids were also prepared. All samples were incubated in the dark at room temperature for 1 h before fluorescence measurements were initiated.

Fluorescence and absorbance measurements

Fluorescence was measured on a SPEX Fluorolog 3 spectrofluorimeter (Jobin-Yvon, Edison, NJ) using quartz semi-micro cuvettes (excitation path length of 10 mm and emission path length of 4 mm). NBD fluorescence was measured at an excitation wavelength of 460 nm and an emission wavelength of 534 nm. Pyrene fluorescence was measured at an excitation wavelength of 350 nm and an emission wavelength of 379 nm. Slit-width bandwidths for fluorescence intensity measurements were set to 4 nm (2 mm physical size) for excitation and emission. The background fluorescence values were <0.02% of that of the sample with fluorophores and were not subtracted. Absorbance was measured using a Beckman 640 spectrophotometer (Beckman Instruments, Fullerton, CA) with quartz cuvettes.

Measurement of the temperature dependence of FRET using two FRET pairs

Samples for FRET experiments were prepared with unlabeled lipids and donor lipid, both with (F samples) and without (Fo samples) acceptor lipids as described above. The donor acceptor FRET pairs were as follows: NBD-DPPE and rhodamine-DOPE (effective Ro in lipid vesicles = 4.9 nm (8)), and pyrene-DPPE and rhodamine-DOPE (effective Ro in lipid vesicles = 2.6 nm (8)). Background samples for Fo samples (containing only unlabeled lipid) and F samples (containing unlabeled lipid plus acceptor, but no donor) were also prepared. Samples were prepared at 70°C and then incubated in the dark at room temperature for 1 h, after which they were cooled to 16°C and the fluorescence measurements were initiated. The cuvette temperature was measured with a probe thermometer (a traceable digital thermometer with a YSI microprobe; Fisher Scientific) dipped inside a sample cuvette before each measurement. The cuvette temperature was increased at a rate of ~0.5°C per minute and readings were taken every 4°C. This process was repeated up to 64°C. The ratio of the average fluorescence intensity in the presence of acceptor to that in its absence (F/Fo) was then calculated. The midpoint transition temperature (T mid) was calculated for each curve. T mid was defined as the point of the maximum slope of a sigmoidal fit of the F/Fo data using Slide Write Plus software (Advanced Graphics Software, Encinitas, CA). For incomplete curves in samples containing 1:1 SM/POPC or 1:1 SM/DOPC with 38% cholesterol, when FRET was detected with the NBD-DPPE/rhodamine-DOPE pair, a limiting value of F/Fo = 0.5 at extremely low temperature was assumed. The T-mid values for these samples were not very sensitive to the exact choice of limiting F/Fo value.

Calculation of donor fluorescence in the presence of acceptor normalized to that in the absence of acceptor (F/Fo)

The approximate F/Fo values that should be obtained as a function of probe partition coefficients and the extent to which large ordered and disordered domains were present in a membrane were calculated using the following equation:

$$\begin{aligned}\mathrm{F/Fo} &= (\mathrm{fr.\,Ld}/[(\mathrm{fr.\,Ld}) + (\mathrm{Kp_d})(1\text{-}\mathrm{fr.\,Ld})])\\ &\left(\exp\left(\left(\text{-}1.21\pi\mathrm{R_o^2C_a}\right)/[\mathrm{fr.Ld} + (1\text{-}\mathrm{fr.\,Ld})(\mathrm{Kp_a})]\right)\right)\\ &+(1\text{-}[\mathrm{fr.\,Ld}/[(\mathrm{fr.\,Ld}) + (\mathrm{Kp_d})(1\text{-}\mathrm{fr.\,Ld})])\\ &\left(\exp\left(\left(\text{-}1.21\pi\mathrm{R_o^2}\right)([(\mathrm{Kp_a})(\mathrm{C_a})]/[\mathrm{fr.Ld} + (1\text{-}\mathrm{fr.\,Ld})(\mathrm{Kp_a})]\right)\right),\end{aligned}$$

where fr.Ld and fr.Lo are the fraction of the bilayer in the form of Ld and Lo domains, respectively; Kp_a and Kp_d are the partition coefficients between Lo and Ld domains for acceptor and donor, respectively (with Kp > 1 indicating preferential location in Lo domains); and C_a is the overall concentration of acceptor in the bilayer molecules/unit area. This equation is derived in the Supporting Material.

RESULTS

FRET assay of domain and ultrananodomain formation

Ultrananodomains were detected by means of a dual-FRET approach in which they were defined as domains that could

be detected with pyrene-DPPE as the donor and rhodamine-DOPE as the acceptor FRET pair (effective Ro = 2.6 nm (8)), but were too small to be detected with the NBD-DPPE as the donor and rhodamine-DOPE as the acceptor FRET pair (effective Ro = 4.9 nm (8)). Domain formation in lipid vesicles containing high-T_m lipid (i.e. with a high gel-to-Ld melting temperature when in a single component lipid bilayer), low-T_m lipid, and cholesterol results in partial segregation of pyrene-DPPE or NBD-DPPE, both of which have a moderate affinity for Lo domains, from rhodamine-DOPE, which strongly partitions into Ld domains (8). This segregation results in weak FRET, and thus strong donor fluorescence, whereas FRET is strong (i.e., donor fluorescence is weak) in homogeneous vesicles lacking membrane domains.

FRET was measured in lipid vesicles composed of these ternary lipid mixtures as a function of increasing temperature. As temperature increases, there tends to be a decrease in domain size, and at sufficiently high temperatures, a total loss of domain formation (8,14). From curves of unquenched donor fluorescence versus temperature, a thermal transition from a state in which domains are present to one in which domains are either lost or too small to detect can be observed. Above the transition temperature, FRET versus temperature levels off to a value equal to that observed in vesicles in a homogeneous Ld phase (8). The midpoint in the sigmoidal unquenched donor fluorescence versus temperature curve, *T* mid, represents the middle of the temperature range over which detectable domain formation is lost. As noted above, for the purposes of this report, we define ultrananodomains as domains that cannot be detected with the NBD-DPPE/rhodamine-DOPE FRET pair, but can be detected with the pyrene-DPPE/rhodamine-DPPE FRET pair. Hence, ultrananodomains are defined as those that are less than ~10 nm in width/diameter, i.e., have a half-width/radius smaller than the effective Ro for the NBD-rhodamine lipid pair in membranes (4.9 nm). This is equivalent to circular domains of ~100 lipids per leaflet (assuming a cross-sectional diameter of 0.8–0.9 nm per lipid molecule). Total domain formation (i.e., on the ultrananodomain size scale and larger) was detected with the pyrene-DPPE/rhodamine-DOPE lipid pair. It should be noted that this pair does not enable detection of domain formation for the smallest ultrananodomains, i.e., those with radius less than the effective Ro (~2.6 nm) for this pair, which corresponds to those with fewer than ~25 lipids per leaflet.

Effect of lipid composition on ultrananodomain formation

Fig. 1 shows the fraction of donor fluorescence that was unquenched by the acceptor (F/Fo) in vesicles composed of 1:1 bSM/POPC with 28 mol % or 38 mol % cholesterol. With the pyrene-rhodamine lipid pair, a clear thermal transition was detected. Below this transition, the vesicles contained coexisting Lo and Ld domains (8,15,16). (Notice

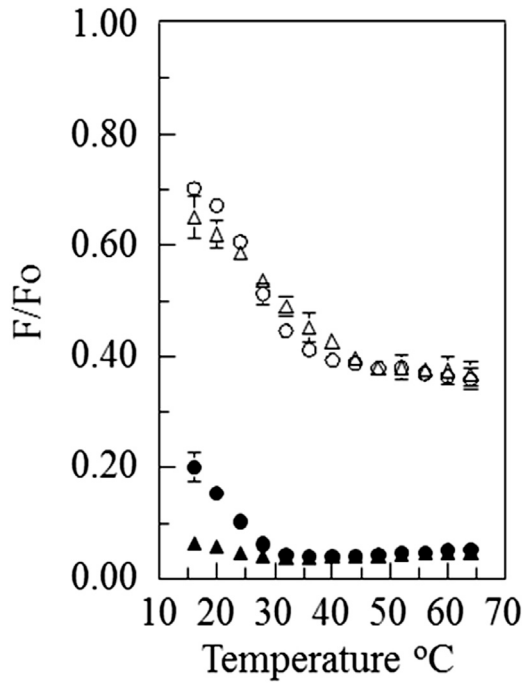

FIGURE 1 Effect of temperature on FRET for vesicles composed of 1:1 bSM/POPC with cholesterol. The samples contained 1:1 SM/POPC with (not correcting for labeled lipids present) 38 mol % (*triangle*) or 28 mol % (*circle*) cholesterol. In all figures, the samples also contained 0.05 mol % pyrene-DPPE (*open symbols*) or 0.1 mol % NBD-DPPE (*solid symbols*) and, when acceptor was present, 2 mol % rhodamine-DOPE. In all figures, the samples contained vesicles with 500 μM total unlabeled lipid dispersed in PBS, pH 7.4. F/Fo equals the ratio of donor (pyrene-DPPE or NBD-DPPE) fluorescence in the presence of acceptor (rhodamine-DOPE) to that in its absence. FRET efficiency is 1-F/Fo. In all figures, standard deviations are shown when they are larger than the symbol size; the number of samples is given in Table 1.

that at high temperature, above the transition to a homogeneous disordered state, there was much less FRET (higher F/Fo) for samples with the pyrene-rhodamine lipid pair than for samples with the NBD-rhodamine lipid pair. This reflects the higher Ro for the latter pair.) Fig. 1 also shows that for the NBD-rhodamine lipid pair, the transition was less apparent and shifted to much lower temperatures. In the most extreme case, with 38 mol % cholesterol, only the upper end of the thermal transition was detected in the experimental temperature range. These results indicate that there is a wide temperature range over which domains are present, as detected by the pyrene-rhodamine FRET pair, but are too small to be detected with the NBD-rhodamine FRET pair, i.e., they are ultrananodomains. Fig. 2 shows a pattern of fluorescence vs. temperature for 1:1 bSM/DOPC with cholesterol that is similar to that observed with vesicles containing a 1:1 bSM/POPC mixture with cholesterol. However, with 28 mol % cholesterol, the thermal transition detected with the NBD-rhodamine lipid pair was shifted to a significantly higher temperature compared with the samples with a 1:1 SM/POPC mixture. This is

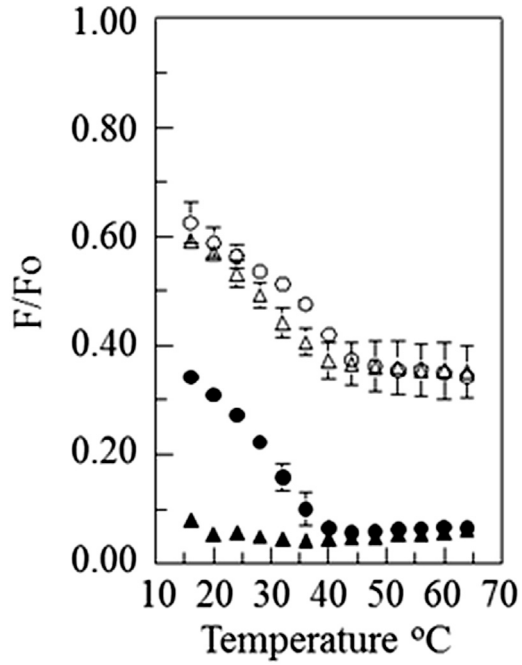

FIGURE 2 FRET versus temperature curves for vesicles composed of 1:1 bSM/DOPC with cholesterol. The samples contained 1:1 SM/DOPC with 38 mol % (*triangle*) or 28 mol % (*circle*) cholesterol. The samples also contained 0.05 mol % pyrene-DPPE (*open symbols*) or 0.1 mol % NBD-DPPE (*solid symbols*) and, when acceptor was present, 2 mol % rhodamine-DOPE.

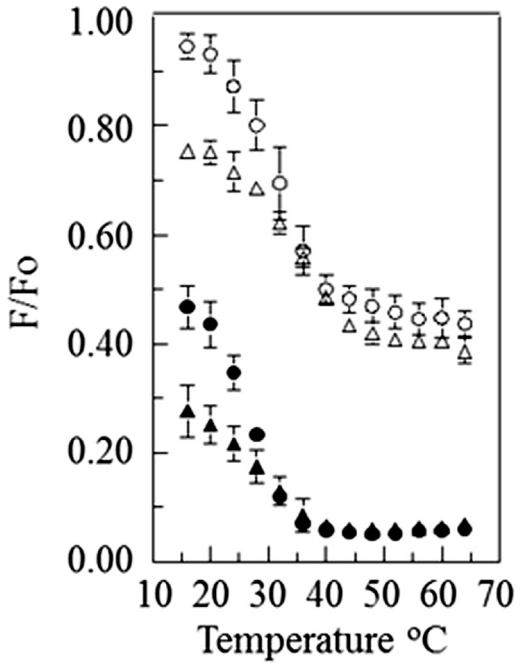

FIGURE 3 FRET versus temperature curves for vesicles composed of 1:1 DPPC/POPC with cholesterol. The samples contained 1:1 DPPC/POPC with 38 mol % (*triangle*) or 28 mol % (*circle*) cholesterol. The samples also contained 0.05 mol % pyrene-DPPE (*open symbols*) or 0.1 mol % NBD-DPPE (*solid symbols*) and, when acceptor was present, 2 mol % rhodamine-DOPE.

indicative of the persistence of domains larger than ultrananodomain size to a higher temperature.

We also obtained F/Fo measurements on vesicles composed of 1:1 DPPC/POPC with 28 mol % or 38 mol % cholesterol (Fig. 3) and 1:1 DPPC/DOPC with 28 mol % or 38 mol % cholesterol (Fig. 4). In contrast to the behavior of vesicles containing bSM, for vesicles containing DPPC, the thermal transition observed with the pyrene-rhodamine lipid pair and the NBD-rhodamine lipid pair occurred over similar temperature ranges. This was true both when the vesicles contained POPC or DOPC and when they contained lower or higher cholesterol concentrations. This indicates that, except over a narrow range of temperatures, the domains that formed in these lipid mixtures were generally larger than ultrananodomains. (It is interesting that the F/Fo values obtained at low temperatures were much higher for pyrene-DPPE in the DPPC/POPC-containing samples than in the DPPC/DOPC-containing samples. This may suggest a higher degree of pyrene-DPPE association with ordered domains, i.e., a partition coefficient favoring the ordered state, in the former samples.)

Table 1 summarizes and quantifies these results in terms of *T* mid, the middle (inflection) point of the transition from a state in which domains that are large enough to be detected are present to one in which domains are either absent or too small to detect with the FRET pair used. The *T*-mid values for the pyrene-rhodamine lipid pair show that the thermal stability of domain formation is similar for vesicles in all of the lipid mixtures studied here. It should also be noted that according to our previous studies (8), the pyrene-rhodamine pair misses the smallest ultrananodomains, and the thermal stability of ordered domain formation in these different mixtures is likely to be somewhat higher and perhaps even more similar than that judged from *T* mid for the pyrene-rhodamine lipid pair (8).

The values listed in Table 1 also show that *T* mid is consistently higher for the pyrene-rhodamine lipid pair than for the NBD-rhodamine pair. This difference indicates that the domain size decreases as the temperature increases in all of the vesicles shown. The relative differences in the tendency to form ultrananodomains versus larger domains can be gauged from the difference between the *T*-mid values for the pyrene-rhodamine lipid FRET pair and the NBD-rhodamine lipid FRET pair (ΔT mid). This roughly reflects the extent of the thermal range over which domains are in the ultrananodomain size range. The larger the gap between T_m values, the greater is the range over which ultrananodomains are present. (Given the way ultrananodomain size is defined above, the actual range over which ultrananodomains are present would begin a few degrees higher than the *T* mid for the NBD-rhodamine lipid pair and end a few degrees higher than the *T* mid for the pyrene-rhodamine lipid pair.) Based on

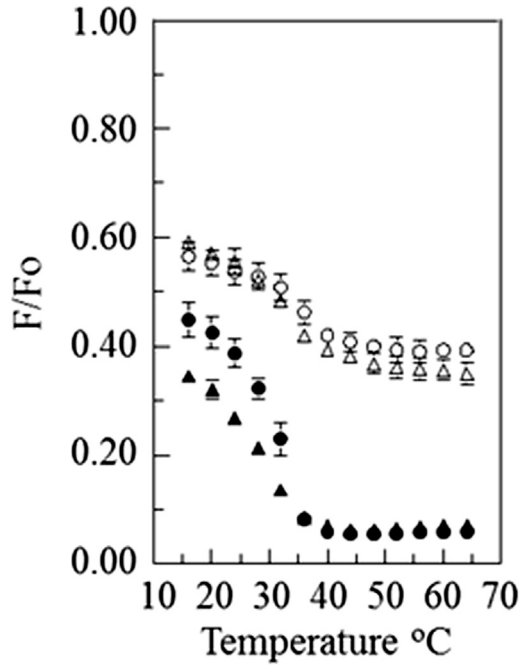

FIGURE 4 FRET versus temperature curves for vesicles composed of 1:1 DPPC/DOPC with cholesterol. The samples contained 1:1 DPPC/DOPC with 38 mol % (*triangle*) or 28 mol % (*circle*) cholesterol. The samples also contained 0.05 mol % pyrene-DPPE (*open symbols*) or 0.1 mol % NBD-DPPE (*solid symbols*) and, when acceptor was present, 2 mol % rhodamine-DOPE.

the Δ*T*-mid values for the NBD-rhodamine pair, ultrananodomain formation over a wide range is favored by bSM, POPC, and higher cholesterol concentrations relative to DPPC, DOPC, and lower cholesterol concentrations, respectively. The *Δ*T-mid values in Table 1 also show that the effect of replacing bSM with DPPC decreases the thermal range over ultrananodomains are present much more than the range is decreased by replacing POPC with DOPC or the range is decreased by replacing 38 mol % cholesterol with 28 mol % cholesterol. In every case, the Δ*T*-mid values indicate that the temperature range over which ultrananodomains form for DPPC-containing vesicles is very small.

DISCUSSION

Using FRET to detect the formation of ultrananodomains

Using FRET with one set of probes with a large Ro value and a second set with a small Ro value should be an excellent way to detect the formation of very small nanodomains, as they should only be detected by the small-Ro probe. However, the actual level of FRET when domains are present is a function of not only domain size but also the fraction of the bilayer in the form of ordered domains, and the partitioning of donor and acceptor between ordered and disordered domains. Since a single acceptor is used, the acceptor partition behavior cannot explain the difference between the FRET obtained using NBD-DPPE as the donor and that obtained using pyrene-DPPE as the donor. Furthermore, with this method, the two donors do not need to have the same affinity for ordered domains (i.e., Kp) or exhibit similar amounts of FRET. Instead, it is only necessary to have two different levels of FRET in the presence or absence of domains. This is because the presence of domains is detected by the change in FRET upon the loss of large domain formation, not from the exact FRET values.

An alternate interpretation of the FRET data could be that NBD-DPPE, but not pyrene-DPPE, is selectively excluded from ordered domains to just the right extent in mixtures rich in SM, POPC, and high cholesterol concentrations and higher temperatures, so as to abolish a change in FRET. This is unlikely, however, as loss of domain detection due to the lack of a change in FRET is only possible at one specific Kp value (see below). More importantly, if lipid packing in ordered domains in the SM/POPC/cholesterol samples is so much tighter than in other lipid mixtures, or the effect of higher temperature is such that it prevents partitioning of NBD-DPPE into the ordered domains, a similar effect on pyrene-DPPE partition would be expected because the pyrene group is larger than NBD and is likely to be at least as disruptive of packing in ordered domains as the NBD group, and this is not observed.

Furthermore, NBD-DPPE has a significant affinity for ordered domains under a wide variety of conditions (8,17,18),

TABLE 1 *T* Mid Values for lipid vesicles of various lipid compositions

High-T_m Lipid	Low-T_m Lipid	Mol % Chol	*T* Mid NBD-Rhodamine	*N*	*T* Mid Pyrene/Rhodamine	*N*	Δ*T* mid
SM	POPC	38	(3.8 ± 2.4)	4	29.7 ± 3.1	4	(25.9)
SM	DOPC	38	(5.6 ± 0.3)	4	28.2 ± 2.8	6	(22.6)
SM	POPC	28	12.9 ± 1.3	4	26.2 ± 0.8	4	13.3
SM	DOPC	28	29.2 ± 1.8	4	33.2 ± 2.6	4	4.0
DPPC	POPC	38	28.1 ± 0.6	4	34.3 ± 0.8	4	6.2
DPPC	DOPC	38	27.9 ± 0.5	4	31.8 ± 0.8	4	3.9
DPPC	POPC	28	26.8 ± 0.5	6	31.3 ± 1.5	4	4.5
DPPC	DOPC	28	30.8 ± 0.3	4	34.7 ± 0.7	4	3.9

Values in parentheses are very rough estimates based on largely incomplete thermal melting curves. *T* mid is defined as the (inflection) point of F/Fo versus temperature curves. Δ*T* mid is *T* mid for the pyrene-DPPE/rhodamine-DOPE FRET pair minus *T* mid for the NBD-DPPE/rhodamine-DPPE pair. Individual *T* mid values were calculated for individual experiments, and averages and standard deviations of *T* mid values are shown.

and although it may not be preferentially located in ordered domains in all conditions (19), this is not a requirement of the FRET studies. As shown in Fig. 5, our calculations (see Supporting Material) indicate that the effect of donor partition on the difference between F/Fo in the presence and absence of domains is highly dependent on the absolute level of FRET. At low levels of FRET (i.e., high F/Fo) when the acceptor partitions strongly into the Ld state (*circles* or *squares*) and domains are large (Fig. 5 *A*), donor fluorescence increases relative to that in the absence of domains (*dashed line*) when domains are present if the donor Kp is >1, and decreases when domains are present if donor Kp is <1. However, the magnitude of the F/Fo change between samples with and without domains is relatively small, ~10–15% of fluorescence in the absence of domains. This can make it difficult to detect domain formation accurately.

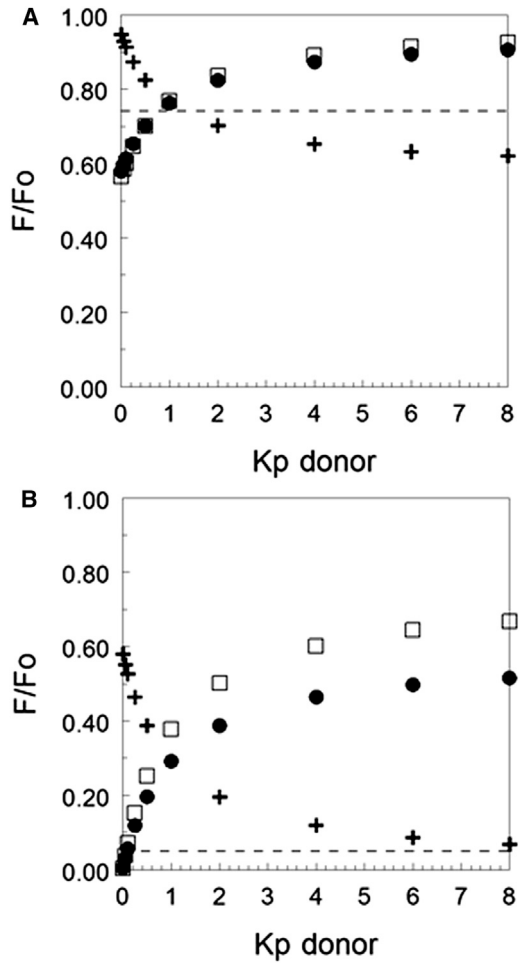

FIGURE 5 Calculated FRET versus donor partition coefficients in domain-containing membranes in which the acceptor partitioned strongly into Ld domains. F/Fo is shown for acceptor Kp (Lo/Ld) values of 0.1 (*circles*), 0.05 (*squares*), and 10 (*plus symbols*). (*A* and *B*) F/Fo is shown at (*A*) low acceptor concentration and/or small-Ro conditions (weak FRET), and (*B*) higher acceptor concentration and/or large-Ro conditions. Panel (*B*) approximates the behavior of the NBD-DPPE/rhodamine-DOPE FRET pair in the experiments (acceptor concentration = 0.79/Ro^2). F/Fo values were calculated for a bilayer that was 50% Lo domains. F/Fo values for homogeneous membranes lacking domains (and/or acceptor Kp = 1) are shown by dashed lines.

The situation is different when an acceptor that partitions strongly into Ld domains is used at a concentration that is sufficient for very strong FRET (i.e., low F/Fo). As shown in Fig. 5 *B*, for a level of FRET in homogeneous bilayers very similar to what we observed (i.e., at very high temperature for the NBD-DPPE/rhodamine-DOPE pair), there is more donor fluorescence when large domains are present even if the donor Kp is substantially less than 1. Furthermore, the increase in F/Fo with domains versus F/Fo without domains is up to 10-fold (or more) rather than above-mentioned increase of 10–15% under conditions of low acceptor concentration. This large increase results from the fact that when domains are present, the weak FRET (weak quenching of donor) due to the low concentration of acceptor in the ordered domains more than balances out the strong FRET (strong quenching of the donor) due to the high concentration of acceptor in the Ld domains. It is noteworthy that to detect no change in F/Fo upon formation of large domains requires a very specific, very low donor Kp value (~0.1) for an acceptor with low Kp. A donor Kp value above or below ~0.1 gives a detectable increase or decrease, respectively, in F/Fo upon domain formation. Thus, when FRET is strong in the absence of domains, it would be hard to achieve conditions in which a significant and easily detected change in FRET is not observed upon domain formation. Similar behavior, although to a somewhat lower degree, is seen at intermediate levels of FRET, i.e., levels that we observed when the donor was pyrene-DPPE (Fig. S2).

Thus, under the conditions we used, whether the donor partitions favorably into the Lo or Ld domains is not critical to detect domain formation. As noted above, to observe increased F/Fo (decreased FRET) upon formation of large domains, Kp must be greater than ~0.1. In a recent study (20), we measured Kp for NBD-DPPE to be in the range of 0.4–0.6 for a variety of SM/DOPC/cholesterol mixtures with ~37% cholesterol. A Kp of 0.6–1 also fits the F/Fo values for the lipid mixtures in the vesicles studied here for reasonable rhodamine-DOPE Kp, close to 0.1–0.2, which is similar to the values we determined previously for NBD-DOPE (20). Thus, the inability to detect domains with FRET by the NBD-DPPE/rhodamine-DPPE pair under conditions in which they could be detected by the pyrene-DPPE/rhodamine-DOPE pair is highly likely to reflect a small domain size rather than a highly lipid-specific and probe-selective effect of membrane composition on the donor Kp.

The fraction of the bilayer in the ordered and disordered states also affects FRET to some degree. However, the effect of Kp on F/Fo is not greatly affected by the exact fraction of the bilayer in the ordered domains over a wide range (Fig. S3). It should be noted the values modeled in Fig. S2 are for a bilayer that is one-half ordered and one-half

disordered, which is close to what is predicted for the compositions we used by the phase diagram of Petruzielo et al. (21). Furthermore, the exact fraction of ordered bilayer is also of less concern here because it would affect FRET for NBD and pyrene in a similar fashion.

Finally, we previously established that changes in FRET and other fluorescence parameters reflect changes in domain size rather than changes in donor partition in lipid mixtures similar to those used in this study (8). For that purpose, in addition to the FRET pairs used here, we employed a third fluorescence probe, DPH, which is known to have a Kp of ~1 (very insensitive to lipid composition) and an intermediate Ro (3.6 nm) relative to NBD and pyrene when rhodamine-DOPE is used as the acceptor. FRET with DPH gave intermediate *T*-mid values relative to the other FRET pairs, consistent with our hypothesis that the domain size decreases as the temperature increases. More importantly, we also used DPH to measure ordered domain formation via additional assays involving very short range, nearest-neighbor interactions, i.e., processes with smaller Ro on the order of 10 Å. This included 1) DPH fluorescence anisotropy, 2) quenching of DPH fluorescence with TEMPO, and 3) quenching of DPH fluorescence with nitroxide-labeled lipids (8). For bSM/POPC/cholesterol 1:1:1, these three methods gave T-mid values much higher than the T-mid value for DPH to rhodamine-DOPE FRET. In other words, these methods indicated the formation of ultrananodomains over a wide temperature range. Since the detecting probe used in each assay was DPH, the value of DPH Kp is not important. Together with the results obtained using the large-Ro and small-Ro FRET pairs, this presents a picture in which the domain size progressively decreases as the temperature increases.

Lipid composition influences ultrananodomain formation

This study shows that vesicles with all of the lipid mixtures formed ultrananodomains over some range of temperatures as the temperature approached the transition in which ordered domains melt. However, the thermal range of ultrananodomain formation was dependent on lipid composition to an even greater extent than was lipid domain formation. This conclusion is based on the observation that vesicles with DPPC, DOPC, and lower cholesterol concentrations formed domains with a thermal stability similar to that of vesicles in which natural SM was substituted for DPPC, POPC was substituted for DOPC, and/or a higher cholesterol concentration was substituted for a lower cholesterol concentration. Nevertheless, these substitutions all favored the formation of ultrananodomains, with ultrananodomain formation being most favorable (i.e., present over the widest range of temperatures) in vesicles containing mixtures of natural SM, POPC, and higher cholesterol concentrations. The latter vesicles come closest, in terms of lipid composition, to the composition of natural mammalian plasma membranes. Thus, it appears that, at least in the absence of proteins, the formation of ultrananodomains should be favored in mammalian plasma membranes. The difference between DPPC and bSM may not be due to differences in their polar groups, but rather to differences in their hydrocarbon chains, as we previously observed the formation of larger domains in 1:1:1 mol/mol egg SM/POPC/cholesterol than in 1:1:1 bSM/POPC/cholesterol (8).

The behavior of the bSM/POPC/cholesterol and bSM/DOPC/cholesterol mixtures we studied are largely consistent with what we observed previously in 1:1:1 bSM/POPC/cholesterol (8), and with the results of Petruzielo et al. (21), who looked at these lipid mixtures over a very wide range of lipid mole fractions. Their studies detected the formation of ultrananodomain-sized domains in bSM/POPC/cholesterol based on FRET and small-angle neutron scattering. However, it is difficult to directly compare the FRET data of Petruzielo et al. with ours. Petruzielo et al. used a low-Ro FRET pair with a high concentration of donor and low concentration of acceptor, and a high-Ro FRET pair with low concentrations of donor and acceptor, whereas we use low donor and higher acceptor concentrations for both low- and high-Ro FRET pairs. Also, they reported relative FRET values and studied acceptor fluorescence enhancement, whereas we measured FRET via donor quenching and obtained absolute values. In any case, Petruzielo et al. described a pattern in which the Ld+Lo coexistence region exhibited domain-induced changes in FRET for the high-Ro pair with both bSM/POPC/chol and bSM/DOPC/chol. At 38 mol % cholesterol, we observed only tiny changes in FRET relative to that found in the absence of domains with the large-Ro pair.

The data of Petruzielo et al. (21) could be interpreted as indicating the formation of domains larger than Ro in 1:1 bSM/DOPC with 38 mol % cholesterol, whereas we report only smaller ones. However, this would be based on the concept that FRET only responds to domains when they are larger than Ro, which is not strictly correct. There is a small difference between FRET for homogeneous and domain-containing membranes when the domains are smaller than Ro, i.e., detecting a small difference in FRET between a sample with no domains and one with domains does not mean the domains are larger than Ro. Thus, it is not clear whether there is any conflict between our data and those of Petruzielo et al. for samples with 38 mol % cholesterol. We believe the protocol we used in our study is particularly efficient for defining domain size using FRET with probes having different Ro values.

It should be noted that based on the FRET behavior of the NBD-rhodamine lipid pair, one can only define a minimum domain size. When the NBD-rhodamine pair indicates that larger domains are present, it does not distinguish between large-scale phase separation and the formation of large nanodomains. These studies also provide no information

about domain shape. The ultrananodomains could be discontinuous Lo or Ld domains, or thin continuous stripes that separate discontinuous domains of the Ld or Lo state, respectively. We also do not know whether any discontinuous domains are nearly circular or highly irregular in shape. Finally, whether or not the domain size observed represents an equilibrium size, which would remain unchanged after a long preincubation of many hours, is not clear. However, given the lipid flux and metabolic activity of cells, it is not clear whether a natural membrane would contain domains at their equilibrium size.

It is noteworthy that the factors that influence domain size on the ultrananodomain scale may be similar to those that affect whether domains are nanodomains or macroscopic. For example, mixtures with POPC tend to make nanodomains, whereas those with DOPC make larger domains (22,23), and egg SM makes macroscopic domains under conditions in which bSM does not (20,24).

Potential biological implications of ultrananodomain formation

We use the term "ultrananodomains" to describe the case in which lipid nanodomains have a particularly small size (in this study, the size is defined by the FRET probes used). It should be pointed out that when the average domain size is larger than the ultrananodomain size, some level of ultrananodomains may be present due to domain size heterogeneity. We also emphasize that we are not stating that domains with an ultrananodomain size are a distinct new species of domain; their formation may just reflect what would happen to the domain/phase size as the composition or temperature approaches the boundary between a two-phase and a one-phase region. Nevertheless, even if ultrananodomains have the same physical properties as macroscopic-sized phases (i.e., act like miniature phases in terms of having distinct properties and differences in affinities for specific lipids and proteins), there could also be important differences in protein behavior between ultrananodomains and larger macroscopic phases. The fact that many or even most of the molecules in an ultrananodomain would remain close to the domain edges could have important functional consequences. A protein at the edge of a domain would be able to interact with a protein outside of the domains, especially if the protein had a large extramembranous domain protruding beyond the domain edge. Also, a protein embedded within an ultrananodomain that is too small to include other proteins would tend to be segregated from other proteins in the same domain type, and thus would not be subject to the enhanced protein-protein interactions that occur when proteins are concentrated in a larger domain. However, the protein would still be affected by the difference between the physical properties of the lipids of the domain (ordered or disordered) with which it is associated, and those of the type of domain with which it is not associated. In this regard, even an ultrananodomain would be sufficient to modulate protein function. A caveat is that a domain would have to persist long enough for a protein to form its equilibrium conformation in that lipid environment. If the lipid environment of a protein fluctuates faster than the protein can change its conformation, it might form an average conformation that reflects its average lipid environment. The extent to which this influences protein behavior is unknown because the persistence time of individual ultrananodomains is unknown. However, the fact that fluorescent lipid quenching due to FRET (and thus fluorescent lipid localization within domains or excluded from domains) is not random indicates that domains persist long enough for fluorescent lipids to establish a near-equilibrium localization. In addition, it is likely that the presence of proteins with strong affinities for Lo or Ld domains could significantly increase the persistence times and sizes of the domains in which they are located by selecting their local lipid environment. In this regard, it is interesting that membrane proteins can increase domain sizes and induce large-scale phase separation (8,25). Of course, there may also be a biological advantage for nanodomains that can rapidly form or disperse in response to specific stimuli.

Taken together, the above considerations indicate that lipid-raft functions that involve protein clustering and segregation may be altered by events that cluster ultrananodomains into larger domains. This could be physiologically important, because domain size appears to be more sensitive to membrane composition, and thus more susceptible to regulation by changes in lipid composition, than is domain formation.

SUPPORTING MATERIAL

Supporting Materials and Methods and three figures are available at http://www.biophysj.org/biophysj/supplemental/S0006-3495(15)00864-4.

AUTHOR CONTRIBUTIONS

P.P. designed the research, performed the research, analyzed data, and co-wrote the manuscript. E.L. designed the research, analyzed data, and co-wrote the manuscript.

ACKNOWLEDGMENTS

This work was supported by National Institutes of Health grant GM 099892.

REFERENCES

1. London, E. 2005. How principles of domain formation in model membranes may explain ambiguities concerning lipid raft formation in cells. *Biochim. Biophys. Acta.* 1746:203–220.
2. Simons, K., and D. Toomre. 2000. Lipid rafts and signal transduction. *Nat. Rev. Mol. Cell Biol.* 1:31–39.

3. Waheed, A. A., and E. O. Freed. 2009. Lipids and membrane microdomains in HIV-1 replication. *Virus Res.* 143:162–176.
4. Brown, D. A., and E. London. 1998. Functions of lipid rafts in biological membranes. *Annu. Rev. Cell Dev. Biol.* 14:111–136.
5. Konyakhina, T. M., S. L. Goh, …, G. W. Feigenson. 2011. Control of a nanoscopic-to-macroscopic transition: modulated phases in four-component DSPC/DOPC/POPC/Chol giant unilamellar vesicles. *Biophys. J.* 101:L8–L10.
6. Feigenson, G. W., and J. T. Buboltz. 2001. Ternary phase diagram of dipalmitoyl-PC/dilauroyl-PC/cholesterol: nanoscopic domain formation driven by cholesterol. *Biophys. J.* 80:2775–2788.
7. Heberle, F. A., R. S. Petruzielo, …, J. Katsaras. 2013. Bilayer thickness mismatch controls domain size in model membranes. *J. Am. Chem. Soc.* 135:6853–6859.
8. Pathak, P., and E. London. 2011. Measurement of lipid nanodomain (raft) formation and size in sphingomyelin/POPC/cholesterol vesicles shows TX-100 and transmembrane helices increase domain size by coalescing preexisting nanodomains but do not induce domain formation. *Biophys. J.* 101:2417–2425.
9. Giang, H., R. Shlomovitz, and M. Schick. 2015. Microemulsions, modulated phases and macroscopic phase separation: a unified picture of rafts. *Essays Biochem.* 57:21–32.
10. Brown, A. C., K. B. Towles, and S. P. Wrenn. 2007. Measuring raft size as a function of membrane composition in PC-based systems: Part II–ternary systems. *Langmuir.* 23:11188–11196.
11. Brown, A. C., K. B. Towles, and S. P. Wrenn. 2007. Measuring raft size as a function of membrane composition in PC-based systems: Part 1–binary systems. *Langmuir.* 23:11180–11187.
12. Towles, K. B., A. C. Brown, …, N. Dan. 2007. Effect of membrane microheterogeneity and domain size on fluorescence resonance energy transfer. *Biophys. J.* 93:655–667.
13. Heberle, F. A., J. T. Buboltz, …, G. W. Feigenson. 2005. Fluorescence methods to detect phase boundaries in lipid bilayer mixtures. *Biochim. Biophys. Acta.* 1746:186–192.
14. Honerkamp-Smith, A. R., P. Cicuta, …, S. L. Keller. 2008. Line tensions, correlation lengths, and critical exponents in lipid membranes near critical points. *Biophys. J.* 95:236–246.
15. Veatch, S. L., and S. L. Keller. 2003. A closer look at the canonical 'raft mixture' in model membrane studies. *Biophys. J.* 84:725–726.
16. Veatch, S. L., and S. L. Keller. 2005. Miscibility phase diagrams of giant vesicles containing sphingomyelin. *Phys. Rev. Lett.* 94:148101.
17. Wan, C., V. Kiessling, and L. K. Tamm. 2008. Coupling of cholesterol-rich lipid phases in asymmetric bilayers. *Biochemistry.* 47:2190–2198.
18. Crane, J. M., and L. K. Tamm. 2004. Role of cholesterol in the formation and nature of lipid rafts in planar and spherical model membranes. *Biophys. J.* 86:2965–2979.
19. Baumgart, T., G. Hunt, …, G. W. Feigenson. 2007. Fluorescence probe partitioning between Lo/Ld phases in lipid membranes. *Biochim. Biophys. Acta.* 1768:2182–2194.
20. Lin, Q., and E. London. 2015. Ordered raft domains induced by outer leaflet sphingomyelin in cholesterol-rich asymmetric vesicles. *Biophys. J.* 108:2212–2222.
21. Petruzielo, R. S., F. A. Heberle, …, G. W. Feigenson. 2013. Phase behavior and domain size in sphingomyelin-containing lipid bilayers. *Biochim. Biophys. Acta.* 1828:1302–1313.
22. Heberle, F. A., J. Wu, …, G. W. Feigenson. 2010. Comparison of three ternary lipid bilayer mixtures: FRET and ESR reveal nanodomains. *Biophys. J.* 99:3309–3318.
23. Zhao, J., J. Wu, …, G. W. Feigenson. 2007. Phase studies of model biomembranes: complex behavior of DSPC/DOPC/cholesterol. *Biochim. Biophys. Acta.* 1768:2764–2776.
24. Visco, I., S. Chiantia, and P. Schwille. 2014. Asymmetric supported lipid bilayer formation via methyl-β-cyclodextrin mediated lipid exchange: influence of asymmetry on lipid dynamics and phase behavior. *Langmuir.* 30:7475–7484.
25. Hammond, A. T., F. A. Heberle, …, G. W. Feigenson. 2005. Crosslinking a lipid raft component triggers liquid ordered-liquid disordered phase separation in model plasma membranes. *Proc. Natl. Acad. Sci. USA.* 102:6320–6325.

Supplementary Material for "The Effect of Membrane Lipid Composition Upon the Formation of Lipid Ultra-Nanodomains" by Pathak, P. and London, E.

Estimating the Effect of Membrane Domain Formation Upon Donor Quenching

In the presence of an acceptor, the concentration dependence of donor quenching in a homogeneous bilayer can be approximated by (Chattopadhyay and London (1987) Biochemistry 26, 39-45):

$$(1)\quad F/Fo = \exp(-1.21\pi R_o^2 C_a)$$

Where C_a is the acceptor concentration in acceptors/area. This expression is strictly valid for a process with very close to an all-or-none distance dependence, and is a good approximation to FRET quenching of donor fluorescence by acceptor within a few percent (Chattopadhyay and London (1987) Biochemistry 26, 39-45). The donor fluorescence in a domain- containing membrane sample is the sum of the donor fluorescence in each domain. For a probe with fluorescence that is not dependent upon lipid phase, fluorescence will be given by:

$$(2)\quad F/Fo = fr.\ D\ Ld\ [\exp(-1.21\pi R_o^2 C_{a\ Ld})] + fr.\ D\ Lo[\exp(-1.21\pi R_o^2 C_{a\ Lo})]$$

Where fr. D Ld is the fraction of the donor in the Ld state, and fr. D Lo is the fraction of the donor in the Lo state, C_{Ld} is the concentration of the acceptor in the Ld domains, and C_{Lo} is the concentration of the acceptor in the Lo domains. The relationship between C_a, C_{Lo} and C_{Ld} is:

$$(3)\quad C_a = (fr.\ Ld)(C_{a\ Ld}) + (fr.\ Lo)(C_{a\ Lo})$$

Where fr. Ld and fr. Lo are the fractions of the bilayer in the Ld and Lo states, respectively. An analogous expression can be written for donor concentrations:

$$(4)\quad C_d = (fr.\ Ld)(C_{d\ Ld}) + (fr.\ Lo)(C_{d\ Lo})$$

The partition coefficients between Lo and Ld domains for acceptor and donor, respectively, are defined as:

$$(5)\quad Kp_a = C_{a\ Lo} / C_{a\ Ld}$$

$$(6)\quad Kp_d = C_{d\ Lo} / C_{d\ Ld}$$

Combining equations (3) and (5), and using the relationship that fr. Ld + fr. Lo = 1 yields the equations:

$$(7)\quad C_{a\ Ld} = C_a / [fr.Ld + (1\text{-}fr.\ Ld)(Kp_a)]$$

$$(8)\quad C_{a\ Lo} = [(Kp_a)(C_a)] / [fr.Ld + (1\text{-}fr.\ Ld)(Kp_a)]$$

Similarly:

(9) $C_{d\ Ld} = C_d /[fr.Ld+(1-fr.\ Ld)(Kp_d)]$

(10) $C_{d\ Lo} = [(Kp_{\ d})(C_d)]/[fr.Ld+(1-fr.\ Ld)(Kp_d)]$

The fraction of the donor in the Ld domains is given by:

(11) $fr.\ D_{Ld} = [(C_{d\ Ld})(fr.\ Ld)]/ [(C_{d\ Ld})(fr.\ Ld)+ (C_{d\ Lo})(fr.\ Lo)]$

Substitution of (9) and (10) into (11) gives:

(12) $fr.\ D_{Ld} = fr.\ Ld/ [(fr.\ Ld)+ (Kp_{\ d})(1-fr.\ Ld)]$

And thus:

(13) $fr.\ D_{Lo} = 1- fr.\ D_{Ld} = 1-[fr.\ Ld/ [(fr.\ Ld)+ (Kp_{\ d})(1-fr.\ Ld)]]$

Substituting (7),(8),(12), and (13) into equation (2) gives the final expression:

(14) $F/Fo = (fr.\ Ld/ [(fr.\ Ld)+ (Kp_{\ d})(1-fr.\ Ld)])\ (exp((-1.21\pi R_o^2 C_a)/[fr.Ld+(1-fr.\ Ld)(Kp_a))+ (1-[fr.\ Ld/ [(fr.\ Ld)+ (Kp_{\ d})(1-fr.\ Ld)])(exp((-1.21\pi R_o^2)([(Kp_{\ a})(C_a)]/[fr.Ld+(1-fr.\ Ld)(Kp_a)]))$

This gives the value of F/Fo as a function of the donor and acceptor partition coefficients, acceptor concentration, and the fraction of the bilayer in the Ld and Lo states.

Supplementary Figure 1: F/Fo data showing sigmoidal curves fit to data for calculation of T mid. A. bSM/POPC/chol, B. bSM/DOPC/chol, C. DPPC/POPC/chol, D. DPPC/DOPC/chol. Samples contained (triangle) 38 mol% or (circle) 28mol% cholesterol. Samples also contained (open symbols) 0.05 mol% pyrene-DPPE or (filled symbols) 0.1 mol% NBD-DPPE, and when acceptor was present 2 mol% rhodamine-DOPE. The sigmoidal fits were calculating using the SlideWrite program (Advanced Graphics Software Inc., Rancho Santa Fe, CA). In samples with NBD-DPPE, bSM, and either POPC or 38% cholesterol curves are very incomplete, and fits were calculated assuming that F/Fo reaches a limiting value of 0.5 at low temperature. In the case of bSM/DOPC/28mol% cholesterol this may have led to a slight underestimate of Tmid.

Supplementary Figure 2: Calculated FRET vs. donor partition coefficients in domain-containing membranes in which acceptor partitions strongly into Ld domains shown at intermediate acceptor concentration and/or intermediate Ro conditions. F/Fo is shown for acceptor Kp (Lo/Ld) values of 0.1 (circles) and 10 (plus symbols). Values chosen to approximate the behavior of the pyrene-DPPE, rhodamine-DOPE FRET pair in the experiments in this report (acceptor conc. $0.79/Ro^2$). F/Fo values calculated for a bilayer that is 50% liquid ordered domains. F/Fo values for homongeneous membranes lacking domains is shown by the dashed line.

Supplementary Figure 3: Calculated FRET vs. donor partition coefficients in domain-containing membranes in which acceptor partitions strongly into Ld domains shown at high acceptor concentration and/or large Ro conditions at different fractions of the bilayer in ordered domains. F/Fo is shown for acceptor Kp (Lo/Ld) values of 0.1 and (plus symbols) 25%, (squares) 50%, or (diamonds) 75% of the bilayer in Lo doamins. Values chosen to approximate the behavior of the NBD-DPPE, rhodamine-DOPE FRET pair in the experiments in this report (acceptor conc. $0.79/Ro^2$). F/Fo values for homongeneous membranes lacking domains is shown by the dashed line.

Supplementary Figure 1:

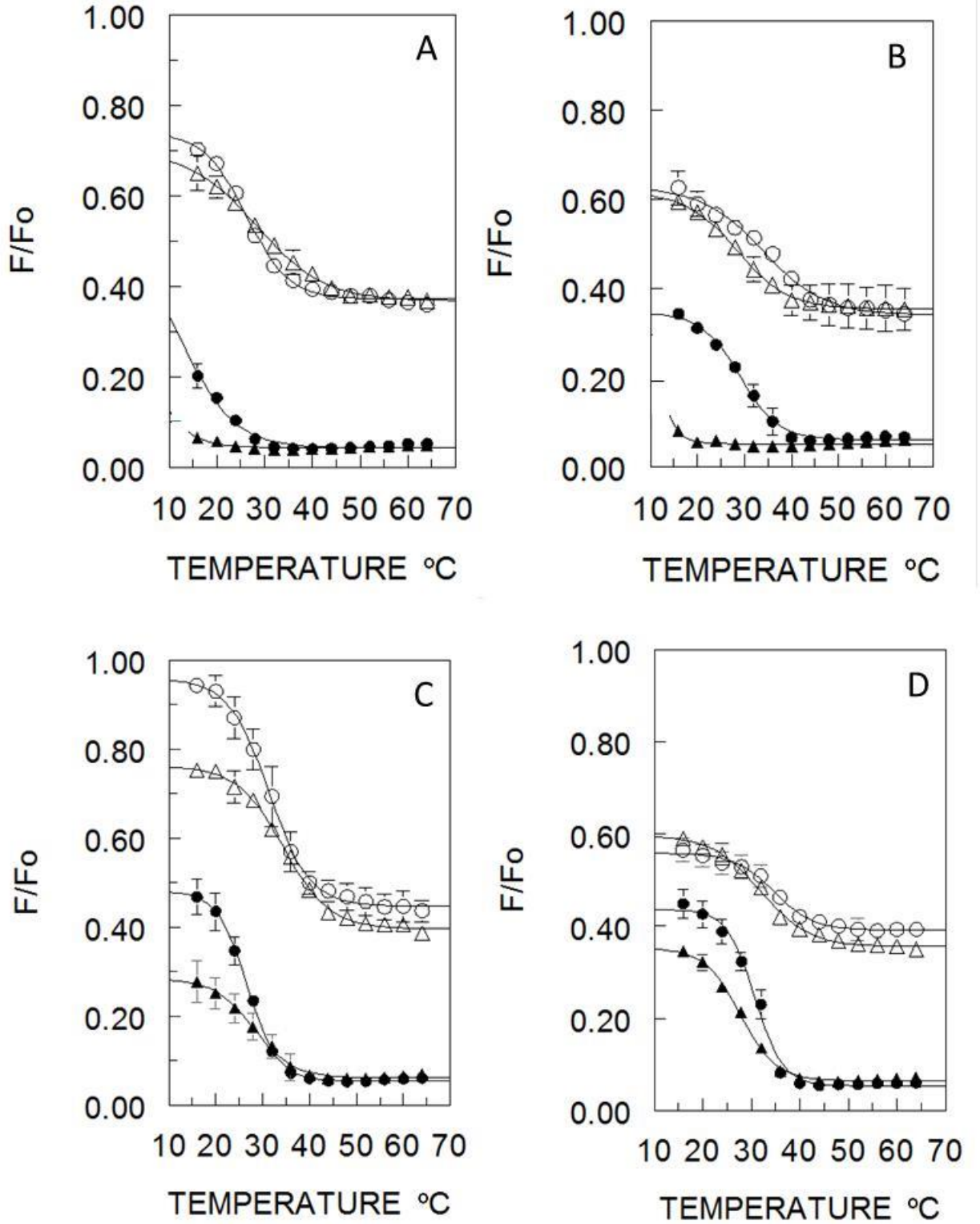

Supplementary Figure 2:

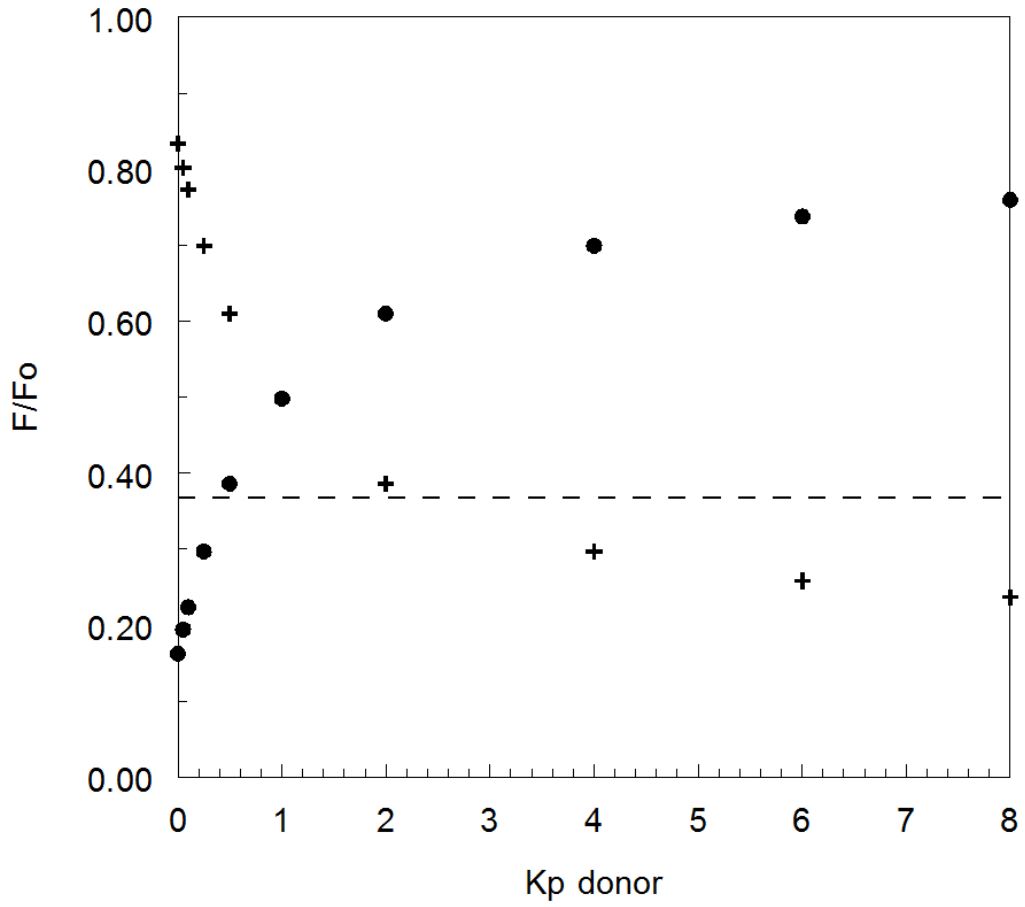

Supplementary Figure 3: